Journal of Renewable Materials

Tech Science Press

DOI: 10.32604/jrm.2023.025871

ARTICLE

Influence of Hydrodynamic Pore Pressure Damage on the Performance of Hot-Mixed Renewable Asphalt Mixture

Guodong Zeng[1], Chao Li[1,*], Yang Fang[1], Hongming Huang[1,2], Hao Li[1,3] and Yishen Xu[1]

[1]Foshan Transportation Science and Technology Co., Ltd., Foshan, 528315, China

[2]Key Laboratory of Road Structure and Material of Ministry of Transport (Changsha), Changsha University of Science & Technology, Changsha, 410114, China

[3]School of Highway Engineering, Chang'an University, Xi'an, 710064, China

[*]Corresponding Author: Chao Li. Email: petrlic@163.com

Received: 03 August 2022 Accepted: 16 September 2022

ABSTRACT

For evaluating the water stability of hot-mixed renewable asphalt mixture (HRM), the traditional methods are all tested under still water conditions. Except for damage in still water conditions, the hydrodynamic pore pressure generated by the tire driving on the surface water has a great impact. Thus, the RAP contents of the HRMs were designed at 0%, 30%, 45% and 60% with AC-25 gradation. Then, the self-designed evaluation methods of water stability and dynamic modulus were studied. Finally, the mechanism of the influence of hydrodynamic pore pressure damage on HRMs was studied. The results show that the water stability of HRM containing 30% RAP is equivalent to that of 45% RAP, and the water stability of HRM containing 60% RAP decreases significantly. The Contabro test after MIST treatment can be used as an evaluation method for hydrodynamic pore pressure damage on HRM. Low-speed, heavy-load traffic and larger RAP content have greater damage to the mixture after hydrodynamic pore pressure damage. The performance differences between the aged bitumen and pure bitumen, as well as the aged minerals and new minerals, are continuing to be enlarged in hydrodynamic pore pressure conditions, finally affecting the water stability and dynamic modulus of the HRMs.

KEYWORDS

Hot-mixed renewable asphalt mixture; water stability; dynamic modulus; hydrodynamic pore pressure

1 Introduction

In the context of energy saving and emission reduction, reclaimed asphalt pavement (RAP) has been increasingly used in highway construction [1,2]. In some hot and rainy areas, the rejuvenating agent is usually not added to hot-mixed renewable asphalt mixture (HRM) [3], because asphalt mixture in these areas does not need great low-temperature performance, and the bitumen that becomes hard and brittle after aging helps to improve high-temperature stability [4,5]. However, the high temperature and rainy conditions require better water stability and viscoelasticity properties of the asphalt mixture.

The bitumen would become hard and brittle after aging [6], which has a certain impact on the water stability of HRM [7,8]. Studies have shown that the early damage to asphalt pavement is intensely related to water damage [2,9]. Water damage has become one of the main reasons for affecting the service life of

asphalt pavement and reducing the service performance of asphalt pavement [10,11]. Therefore, the evaluation of the water stability of HRM is particularly important.

At present, the evaluation methods for the water stability of HRM are mainly freeze-thaw splitting [12], immersion Marshall test [13] and Cantabro test [14]. Based on freeze-thaw splitting tests, Chen et al. [3] studied the impact of RAP content on the water stability of HRM. Results indicated that the water stability of HRMs improved with the addition of RAP. The dynamic modulus was much larger than that of the ordinary asphalt mixture with no RAP. The dynamic modulus of renewable materials with a RAP content of 30% was the largest. Katla et al. [15] adopted the Cantabro test to evaluate the water stability of bituminous mixtures with three fractionation levels and different percentages of RAP. The results showed that there was a good relationship between the Cantabro loss and the evaluation of water stability. Loria et al. [16] studied the resistance to water damage of HRM with high RAP content (up to 50%). Results showed that HRM with 50% RAP could achieve acceptable resistance to water damage, and the use of multiple freeze-thaw cycles provided a better characterization of the HRMs' resistance to water damage.

To sum up, the freeze-thaw splitting test [17], Cantabro test [18] and water immersion Marshall test [19] are simple, effective and widely used, but their test conditions are all based on the water damage of asphalt pavement in still water [20]. Except for damage in still water conditions, during the actual service process of the road surface after rain, the hydrodynamic pore pressure generated by the tire driving on the surface water has a great impact on the asphalt mixture, continuously eroding the mixture gap and surface asphalt mortar. Especially, the influence of RAP on the performance of HRMs under hydrodynamic pore pressure needs to be improved.

In response to these problems, this paper prepared various HRMs with different RAP contents firstly. Secondly, based on water induced sensitivity tester (MIST) [21] and ASTM D7870 [22], self-designed testing methods under hydrodynamic pore pressure damage, were applied to evaluate the effects of RAP content on the water stability. Also, complex modulus tests were carried out on HRMs before and after hydrodynamic pore pressure damage. Finally, in order to analyze the mechanism of hydrodynamic pore pressure damage on HRMs, the performance of bitumen, minerals and structure were analyzed.

2 Materials and Methods

2.1 Raw Materials

The pure bitumen used in the research was 60/80 penetration grade bitumen, and the basic properties were shown in Table 1.

Table 1: Basic properties of pure bitumen

Properties	Units	Results	Requirements [23]	Test methods
Penetration (25°C)	0.1 mm	69	60 > 80	ASTM D5
Penetration index	—	0.913	−1.5 > +1.0	
Softening point	°C	47.5	≥47	ASTM D36
Ductility (10°C)	cm	21	≥15	ASTM D113
Density (25°C)	g/cm^3	1.030	—	ASTM D70
Viscosity (135°C)	Pa·s	0.489	≤3	ASTM D4402
Residue after TFOT				
Mass loss	%	−0.126	−0.8 > +0.8	ASTM D 2872
Penetration ratio (25°C)	%	65	≥61	ASTM D5
Ductility (10°C)	cm	7	≥6	ASTM D113

Coarse aggregates were obtained by crushing limestone with specifications of 3–5 mm, 5–10 mm, 10–15 mm, 10–20 mm and 10–25 mm. Fine aggregate was stone chips of 0–3 mm, and filler was mineral powder obtained by grinding limestone. The properties of aggregates and fillers all met the specification requirements. The used RAP was the milling waste produced by highway maintenance, and the properties were shown in Table 2.

Table 2: Properties of RAP

Properties	Units	Results				Requirements [23]	Test methods
		0–8 mm	8–13 mm	13–19 mm	19–25 mm		
Bitumen content	%	5.63	3.21	2.69	3.17	—	ASTM D2172
Apparent specific density	—	2.649	2.659	2.677	2.701	≥2.600	ASTM C127
Water absorption	%	1.1	1	0.9	0.7	≤2.0	

2.2 Experimental Methods

2.2.1 Preparation of Asphalt Mixture

AC-25 gradation was adopted to design four types of HRMs, the mixtures with RAP content of 0%, 30%, 45% and 60%, were named as HRM-0, HRM-30, HRM-45, HRM-60, respectively. Through experiments on raw materials, it was found that 3.6% was the optimum bitumen content for HRM-0 prepared according to the gradation curve in Fig. 1.

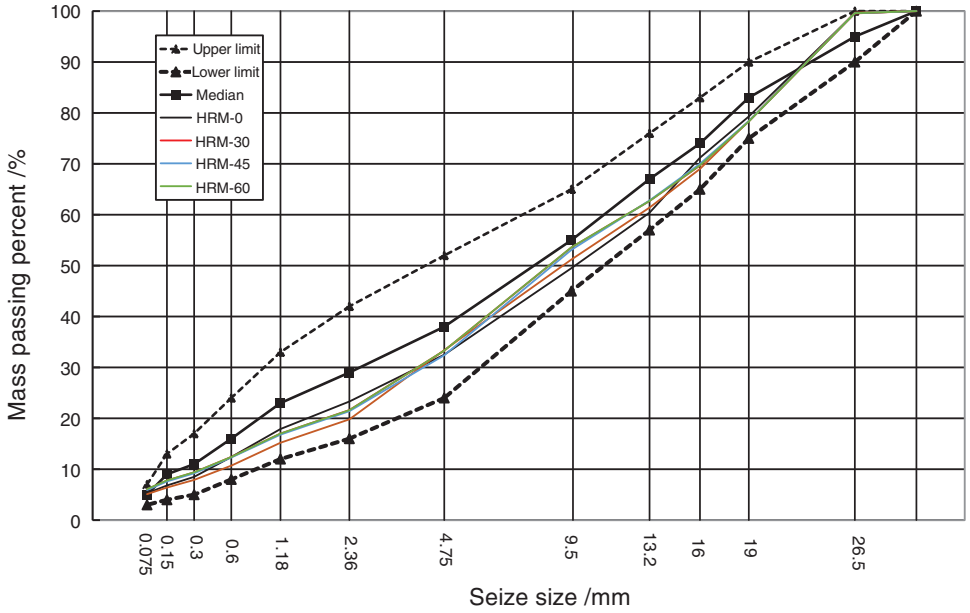

Figure 1: Gradation curves of asphalt mixtures

In order to allow all HRMs to compare the effect of RAP content on performance under the same bitumen contents and similar gradation curves, the bitumen contents of HRM-30, HRM-45 and HRM-60 were all selected as 3.6%, the ratio of aged bitumen in RAP and pure bitumen for HRMs are shown in Table 3, the gradation curves are shown in Fig. 1. Based on the former results, the weight of

mineral part in each grade of RAP can be obtained. According to the bitumen content of different RAP in Table 3, the contents of different grades of RAP were determined.

Table 3: Content of bitumen

Type	HAM-0	HAM-30	HAM-45	HAM-60
Content of aged bitumen (%)	0	1.2	1.6	2.1
Content of pure bitumen (%)	3.6	2.4	2.0	1.5

The preparation process of HRM was shown below: pure bitumen and RAP were preheated at 145°C and 125°C for 2 h, and aggregates were preheated at 190°C for 4 h firstly. Then, RAP and aggregates were mixed at 160°C for 90 s, then pure bitumen was added and mixed for 180 s. After former procedures, HRMs were prepared and could be used to form samples for different tests.

2.2.2 Cantabro Test

Different types of HRMs were formed as Marshall samples firstly, then based on the test methods from T0733-2011, the standard Cantabro test and the immersion Cantabro test were applied to study the water stability of HRMs in still water. In addition, to detect the effects of hydrodynamic pore pressure on the water stability of HRMs, self-designed evaluation method was conducted as follows: the Marshall samples were treated in standard MIST process (60°C, 40 PSI, and 3500 cycles) shown in Fig. 2, and then conducted the standard Cantabro test.

Figure 2: Moisture induced stress tester (MIST)

2.2.3 Dynamic Modulus

Based on AASHTO TP62-03, the effects of hydrodynamic pore pressure damage on the dynamic modulus of HRMs were evaluated. Cylindrical specimens with a diameter of 150 mm and a height of 170 mm were formed by rotary compaction, and the samples with a diameter of 100 mm and a height of 150 mm were drilled. The samples of the mixture were divided into two groups: the first group was not treated, and the second group was treated in standard MIST process (60°C, 40 PSI, and 3500 cycles). The dynamic modulus tests were carried out by using the UTM 100 produced by the IPC Company, Australia. The test temperature was 50°C, and the loading frequencies were 0.1, 0.5, 1, 5, 10 and 25 Hz. The test process is shown in Fig. 3.

Figure 3: Dynamic modulus test

2.2.4 Mechanism Exploration

The elemental compositions of the aged minerals extracted from RAP were analyzed by Shimadzu XRF-1800 X-ray fluorescence spectrometer, and the phase compositions were analyzed by Japan Rigaku SmartLab 9 kW X-ray. The bitumen of HRM-0, HRM-30, HRM-45 and HRM-60 were extracted firstly. Penetration, softening point, and ductility were tested on the obtained bitumen, as well as aged bitumen extracted from RAP.

3 Results and Discussions

3.1 Cantabro Test

3.1.1 Appearance Change

MIST has a built-in pressure chamber. During the test, by continuously injecting and pumping water into the pressure chamber, the hydrodynamic pore pressure was produced by air pressure and water squeezing, thereby simulating the interaction between the wheel and the wet road surface [24]. By adjusting the water temperature and air pressure, the device could simulate hydrodynamic pore pressure and squeezing effect inside the asphalt pavement under different conditions [25]. The MIST test process were shown in Fig. 4.

It can be seen from the Fig. 4 that after the test, there is no debris washed down from the bottom of the pressure chamber, indicating that the Marshall specimen placed in the MIST did not drop particles during the

test. The appearances of all the Marshall specimens are consistent with the appearance of the standard Cantabro test and the immersion Cantabro test after curing, indicating that the three treatment methods have no effects on the appearance of the mixture.

(1) Pressure chamber before test

(2) Pressure chamber after test

(3) Sample before MIST treatment

(4) Sample after MIST treatment

Figure 4: MIST test procedure

3.1.2 Cantabro Loss

In order to study the influence of the MIST test on the water stability, different mixtures were subjected to standard Cantabro test, immersion Cantabro test and standard Cantabro test after MIST. The results are shown in Fig. 5.

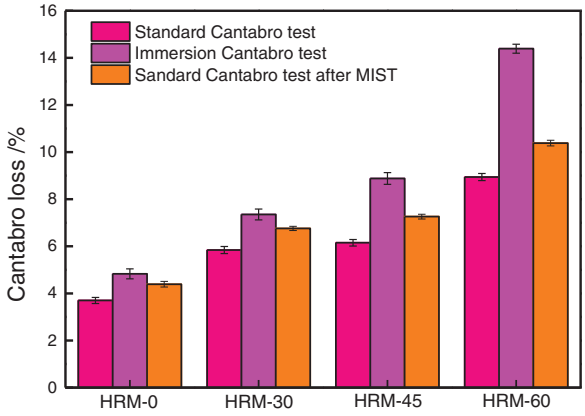

Figure 5: Cantabro test results

As can be seen from Fig. 5, for the same asphalt mixture, the Cantabro loss of the standard Cantabro test is the smallest, followed by the standard Cantabro test after MIST, and finally the immersion Cantabro test. The Cantabro loss under the standard Cantabro test after MIST is not as large as the immersion Cantabro test, which is mainly because the immersion Cantabro test required the sample to be treated in hot water at 60°C for 48 h, while the MIST only needed to treat the sample in hot water at 60°C for 5 h. Despite the hydrodynamic pore pressure damage in MIST, the nearly 10-fold difference in treatment time made the Cantabro loss under the dynamic water pressure not as large as the immersion Cantabro test.

With the increase of RAP content, the Cantabro loss values of the three treatments gradually increase, and the Cantabro loss of immersion Cantabro test increases the fastest. The Cantabro loss of HRM-60 exceeds 14% after immersion Cantabro test, and the water stability decreases significantly.

The variation trend of the Cantabro loss of the standard Cantabro test after MIST treatment is consistent with that of immersion Cantabro test, and the relationship between them is shown in Fig. 6.

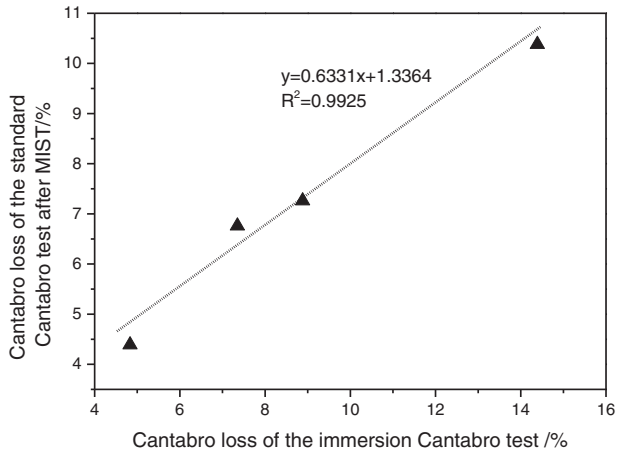

Figure 6: Relationship between the Cantabro loss of the standard Cantabro test after MIST treatment and immersion Cantabro test

As shown in Fig. 6, the relationship between them can be fitted according to the following publicity. $y = 0.6331x + 1.3364$, where: x—the Cantabro loss of the immersion Cantabro test (%), y—the Cantabro loss of the standard Cantabro test after MIST treatment (%). It can be seen from the formula that the relationships are linearly correlated, and the formula fitting degree (R^2) is 0.9925, showing a good correlation.

The whole process of the standard Cantabro test after MIST treatment takes about 25 h (MIST treatment for 5 h + Cantabro test for 20 h), which is only one third of the time of immersion Cantabro test (48 h curing + test for 24 h), so the standard Cantabro test after MIST treatment can be used as an evaluation method for water stability of HRM. This method can simulate the action of hydrodynamic pressure, and evaluate the water stability of the mixture more realistically.

3.2 Dynamic Modulus

As a viscoelastic material, asphalt mixture will show different mechanical properties with the change of temperature and frequency, such as dynamic modulus [26]. Among the four types of asphalt mixtures in this study, the differences in properties and skeleton structure increased with the RAP content. Under the same test conditions, asphalt mixtures can show different orientations between viscous and elastic properties. The dynamic modulus results before MIST processing are shown in Fig. 7.

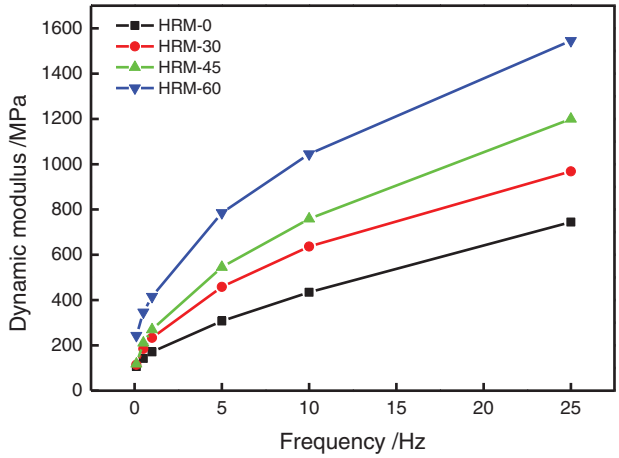

Figure 7: Dynamic modulus before MIST treatment

As can be seen from Fig. 7, all four asphalt mixtures exhibit typical viscoelastic properties. As the loading frequency increases, the energy accumulated in the asphalt mixture cannot be released in a short time, resulting in a gradual increase of the dynamic modulus. At the beginning of loading, the dynamic modulus increases rapidly, and then the growth gradually slows down. This is because the frequency is lower at the beginning of loading, and the impact of bitumen on the entire mixture system is greater, and the mixture exhibits viscous deformation after loading. With the growth of the frequency, the influence of the aggregate on the whole mixture system gradually increased, and the mixture showed elastic deformation after loading.

At the same frequency, the dynamic modulus of HAM-0 is the lowest, and the dynamic modulus increases with the increase of RAP content, but the increasing trend gradually becomes slower with the increase of frequency. When the loading frequency is 25 Hz, the dynamic modulus of HAM-60 has reached more than twice that of HAM-0. The results of the dynamic modulus test of the mixture after MIST treatment are shown in Fig. 8.

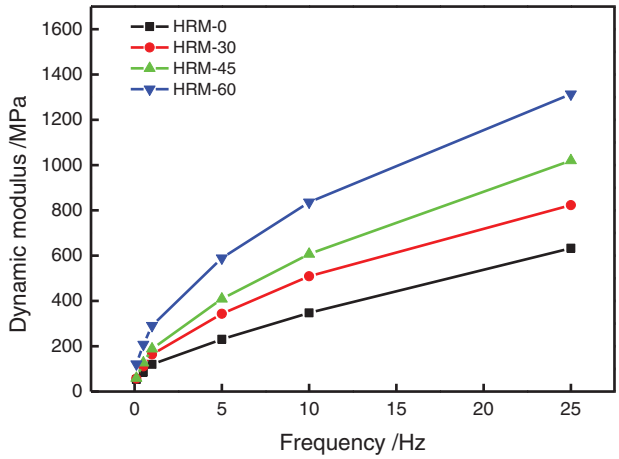

Figure 8: Dynamic modulus after MIST treatment

It can be seen from Fig. 8 that the dynamic modulus of all mixtures shows a decreasing trend after MIST treatment. For the same kind of mixture, with the increase in frequency, the dynamic modulus still shows an increasing trend. When the frequency is low, the increase rate is larger, and the increase rate decreases when

the frequency increases. Compared with the results before the MIST treatment, for the same mixture, the loss of dynamic modulus at low frequency is greater than that at high frequency. So in actual road conditions, low-speed and heavy-load traffic have greater damage to the mixture after hydrodynamic pore pressure damage.

With the increase of RAP content, the decrease of dynamic modulus after MIST treatment increases gradually, because with the increasing proportion of RAP in the mixture, the aging degree of bitumen in the mixture increases. The combination of new and aged bitumen is weaker than the bond between the pure bitumen, leading to the loss of mechanical properties after the hydrodynamic pore pressure damage.

3.3 Mechanism Exploration

Researches have indicated that gradation [27], bitumen [28] and mineral [29], were the main factors affecting water stability and viscoelasticity. Under the same gradation of different mixtures, bitumen and mineral had a greater impact on performance after hydrodynamic pore pressure damage. In addition, changes in asphalt mixture structure during testing may also be reflected in performance differences.

3.3.1 Mineral Characteristics

To study the performance of bitumen in HRMs, aged minerals were extracted from RAP. It was found that there were particles of different colors and textures in the aged minerals, and the picture was shown in Fig. 9.

Figure 9: Extracted aged minerals

In order to analyze the phase composition of different minerals, the particles with similar color and texture were selected. Shapes of sorted aged minerals are shown in the Fig. 10.

It can be seen from Fig. 10 that the aged minerals can be divided into four categories and the descriptions of each category are as follows: (1) This content is the largest, accounting for about 50% of the total minerals, whose color is dark gray, and the surface is rough and hard; (2) This content is the second largest, accounting for about 30% of the total mineral material, whose color is light yellow, the surface is rough and contains more shiny crystalline substances, and the texture is average; (3) This content is the third largest, accounting for about 15% of the total mineral material, whose color is light yellow, the surface is smooth; (4) This content is the least, accounting for about 5% of the total mineral material, whose color is light gray, the surface is smooth and contains pores. In order to further analyze the composition of different colors of aged minerals, four kinds of aged minerals were tested by XRF, and the results are shown in Table 4.

Figure 10: Sorted aged minerals

Table 4: XRF results

The first												
Element type	Ca	O	C	Fe	Si	Al	Zn	Mg	K	Ti	Sr	Na
Content (%)	48.09	20.59	17.01	4.41	3.79	1.69	1.08	0.99	0.64	0.56	0.55	0.30
The second												
Element type	Si	O	Al	K	Ca	Fe	Zn	Na	Mg	Ti	Rb	S
Content (%)	35.79	23.31	11.98	11.31	7.03	4.76	3.02	1.22	0.50	0.47	0.19	0.13
The third												
Element type	Ca	O	C	Si	Mg	Al	Fe	K	Zn	Sr	Ti	S
Content (%)	54.39	22.70	16.62	2.32	1.16	0.95	0.69	0.43	0.35	0.24	0.09	0.05
The fourth												
Element type	Ca	O	C	Si	Al	Fe	K	Mg	Zn	Sr	Ti	Na
Content (%)	45.29	19.21	16.85	8.87	3.28	2.78	1.18	1.03	0.42	0.42	0.27	0.26

It can be seen that the composition of the first, third and fourth aged minerals are relatively similar, and the main components are Ca, O, C, etc., of which the content of Ca is the most, accounting for more than 30% of the total element content. The composition of the second kind of aged mineral is obviously different from that of the first, third and fourth aged mineral. For the specific phase composition of the four aged minerals, XRD phase composition analysis should be carried out according to the element detection results, and the detection results are shown in Fig. 11.

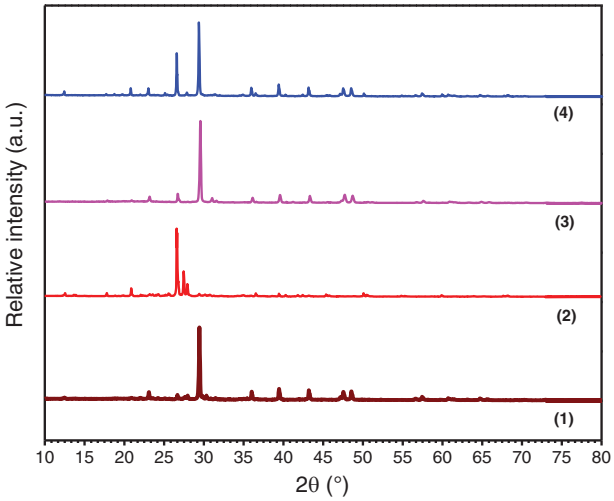

Figure 11: XRD results

According to the Fig. 11 and the comparison with the standard PDF card, it is found that the main phase composition of the first, third and fourth kinds of aged minerals is $CaCO_3$, and the lithological composition is limestone. The composition of the second aged mineral is $CaCO_3$ and SiO_2, and the lithological composition is granite. The crushing value and elongated particles tests were carried out on the aged minerals and the new limestone, the results are shown in the Table 5.

Table 5: Crushing value and elongated particles test results

Properties	Values (%)		Requirement (%) [23]	Test methods
	Aged mineral	Limestone		
Crushing value	20.0	15.5	≤28	BS 812
Needle flake	11.9	7.8	≤18	ASTM D4791–95

As can be seen from Table 5, the crushing value and the elongated particles of the aged minerals and limestone meet the requirements, and the two indicators of the aged minerals are inferior to those of the new limestone. Compared with limestone, the crushing value of the aged minerals increases by 29.03%, and the mechanical properties decrease greatly. This is mainly because during the service process, the RAP would be continuously compacted by the vehicle load, and the milling machine would also destroy the structural properties of the aged minerals in the process of recycling RAP. In addition, Wu studied the interfacial adhesion properties of asphalt, limestone, and granite. The results revealed that the limestone aggregate had a better bond to the asphalt than that of granite aggregate [30]. Thus, the granite composition in the aged minerals also affects the overall mechanical properties and crush resistance of the aggregate.

3.3.2 Bitumen Characteristics

In order to study the performance of bitumen in HRMs, penetration, softening point and ductility tests were carried out on different types of bitumen extracted from HRMs, and the results are shown in Table 6.

Table 6 shows that with the increase of RAP content, it is found that with the increase of RAP content, the penetration gradually decreases, the softening point gradually increases, and the ductility decreases rapidly. The softening point and ductility at 15°C of HRM-30 can also meet the technical indicators of

pure bitumen. Among the three major indicators of HRM-45 and HRM-60, only the softening point can meet the technical indicators of pure bitumen.

Table 6: Test results of conventional properties of bitumen

Properties	Units	Samples					Test methods
		HRM-0	HRM-30	HRM-45	HRM-60	Aged bitumen	
Penetration (25°C)	0.1 mm	60	46	35	26	23	ASTM D5
Softening point	°C	48.1	50.5	56.9	61.3	68	ASTM D36
Ductility (15°C)	cm	>100	>100	22	5	0.5	ASTM D113

3.3.3 Structure Characteristics

In order to study the influence of hydrodynamic pore pressure on the structure of the mixture, the bulk specific density and percent air void of the Marshall specimens before and after MIST treatment were tested, and the results are shown in Table 7.

Table 7: The bulk specific density and percent air void before and after MIST treatment

Properties		Unit	HRM-0	HRM-30	HRM-45	HRM-60	Test methods
Theoretical maximum relative density		—	2.551	2.529	2.509	2.496	ASTM D2041
Before MIST	Bulk specific density	—	2.414	2.400	2.392	2.382	ASTM 2726
	Percent air void	%	5.4	5.1	4.6	4.5	
After MIST	Bulk specific density	—	2.382	2.374	2.370	2.367	
	Percent air void	%	6.6	6.1	5.5	5.1	

From Table 7, with the increase of RAP content, the theoretical maximum relative density of the mixture gradually decreases, which is caused by the lower density of the aged minerals in RAP used in this study. For the same asphalt mixture, after MIST treatment, Marshall specimens show a trend of decreasing bulk specific density and increasing percent air void. In the pressure chamber of MIST, water injection and pumping were repeated continuously, and the hydrodynamic pore pressure was stimulated by air and water pressure, which continuously squeezed the specimen. The structure of the specimen has been damaged by the influence of the hydrodynamic pore pressure, resulting in the increase of the open and closed voids of asphalt mixtures.

In summary, although previous studies have shown that the water stability [31] and viscoelastic [3] properties of HRMs were better than those of new asphalt mixtures, the results in this paper did not show the same conclusions because of the differences in the experimental environment. As shown in Fig. 12, the main reason is that under still water test conditions, the structure of the mixture will not be greatly affected, and the aged bitumen helps HRMs to show better water stability and viscoelasticity. However, under the test conditions of MIST, the hydrodynamic pore pressure caused by air pressure and water squeezing will continuously impact the structure of the mixture. The performance differences between the aged bitumen and pure bitumen, as well as the aged minerals and new minerals, are continuous to be enlarged in hydrodynamic pore pressure conditions, which will eventually destroy the structure during testing, finally affecting the water stability and dynamic modulus of the HRMs.

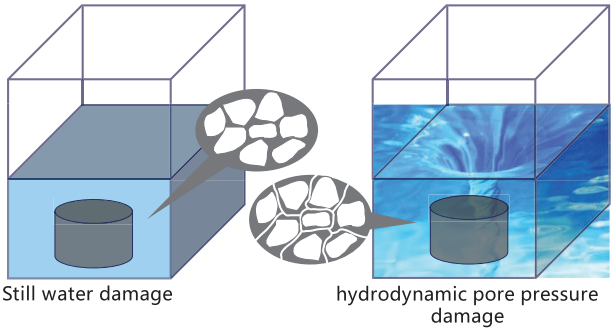

Figure 12: Schematic diagram of water damage

4 Conclusions

In order to study the HRMs' water stability and dynamic modulus after hydrodynamic pore pressure damage treated by the water-induced stress tester (MIST), the RAP content of the HRMs was designed at 0%, 30%, 45% and 60% with AC-25 gradation. Then, the self-designed evaluation methods of water stability and dynamic modulus were used to study the effects of hydrodynamic pore pressure damage on the performance of HRMs. Finally, based on the performance of bitumen, minerals and structure, the mechanism of the influence of hydrodynamic pore pressure damage on HRMs was studied. The following conclusions can be drawn:

(1) The standard Contabro test after MIST treatment can be used as an evaluation method for water stability under hydrodynamic pore pressure damage. With the increase of RAP content, the water stability of HRMs under hydrodynamic pore pressure damage decreased continuously.

(2) The decrease of dynamic modulus after MIST treatment increases gradually with the augment of RAP content. Low-speed, heavy-load traffic and larger RAP content have greater damage to the mixture after hydrodynamic pore pressure damage.

(3) The performance differences between the aged bitumen and pure bitumen, as well as the aged minerals and new minerals, are continuing to be enlarged in hydrodynamic pore pressure conditions, which will eventually destroy the structure during testing, finally affecting the water stability and dynamic modulus of the HRMs.

Acknowledgement: The authors thank the materials and experimental instruments supported by Foshan Transportation Science and Technology Co., Ltd.

Funding Statement: This work was financially by the Self-Financing Technology Plan Project of Foshan (2020001005386).

Conflicts of Interest: The authors declare that they have no known competing financial interests or personal relationships that could have appeared to influence the work reported in this paper.

References

1. Abdalfattah, I. A., Mogawer, W. S., Stuart, K. (2021). Quantification of the degree of blending in hot-mix asphalt (HMA) with reclaimed asphalt pavement (RAP) using energy dispersive X-ray spectroscopy (EDX) analysis. *Journal of Cleaner Production, 294,* 126261. DOI 10.1016/j.jclepro.2021.126261.
2. Austerman, A. J., Mogawer, W. S., Stuart, K. D. (2020). Variability of reclaimed asphalt pavement (RAP) properties within a state and its effects on RAP specifications. *Transportation Research Record, 2674(6),* 73–84. DOI 10.1177/0361198120917679.

3. Chen, Y. H., Chen, Z. G., Xiang, Q., Qin, W. J., Yi, J. Y. (2021). Research on the influence of RAP and aged asphalt on the performance of plant-mixed hot recycled asphalt mixture and blended asphalt. *Case Studies in Construction Matrials, 15,* e00722. DOI 10.1016/j.cscm.2021.e00722.
4. Al-Saffar, Z. H., Yaacob, H., Satar, M. K. I. M., Saleem, M. K., Lai, J. C. et al. (2021). A review on rejuvenating materials used with reclaimed hot mix asphalt. *Canadian Journal of Civil Engineering, 48,* 233–249. DOI 10.1139/cjce-2019-0635.
5. Zhang, K., Huchet, F., Hobbs, A. (2019). A review of thermal processes in the production and their influences on performance of asphalt mixtures with reclaimed asphalt pavement (RAP). *Construction and Building Materials, 206,* 609–619. DOI 10.1016/j.conbuildmat.2019.02.057.
6. Hja, B., Mmk, C., Hn, B., Fmn, B. (2020). Sustainable asphalt concrete containing high reclaimed asphalt pavements and recycling agents: Performance assessment, cost analysis, and environmental impact. *Journal of Cleaner Production, 244,* 118337.
7. Radeef, H. R. (2021). A review on the durability of recycled asphalt mixtures embraced with rejuvenators. *Sustainability, 13(16),* 8970. DOI 10.3390/su13168970.
8. Prosperi, E., Bocci, E. (2021). A review on bitumen aging and rejuvenation chemistry: Processes, materials and analyses. *Sustainability, 13(12),* 6523.
9. Falchetto, A. C., Moon, K. H., Kim, D. H. (2020). Evaluation of recycled asphalt mixture at low temperature using different analytical solutions. *Canadian Journal of Civil Engineering, 47(7),* 801–811. DOI 10.1139/cjce-2019-0303.
10. Pasandín, A., Pérez, I., Gómez-Meijide, B. (2020). Performance of high rap half-warm mix asphalt. *Sustainability, 12(24),* 10240. DOI 10.3390/su122410240.
11. Zhou, Z., Liu, X., Luo, S., Sha, X. (2016). Effect of water intrusion on performance of asphalt mixture. *Journal of Central South University (Science and Technology), 5(9),* 180–183.
12. He, Z. Y., Chen, L., Chen, X. Y., Cheng, Y. (2016). Mechanical properties and application research of hot recycled asphalt mixture from central mixing plant. *Journal of Building Materials, 18(5),* 50–52.
13. Zhu, J., Ma, T., Cheng, H., Li, T., Fu, J. (2021). Mechanical properties of high-modulus asphalt concrete containing recycled asphalt pavement: A parametric study. *Journal of Materials in Civil Engineering, 33(5),* 04021056. DOI 10.1061/(ASCE)MT.1943-5533.0003678.
14. Sun, Z. H., Wang, T. B., Wu, Z. F., Wang, Z. S. (2014). Research on the evaluation method of water stability for large size aggregate particle asphalt mixture. *Applied Mechanics and Materials, 692,* 497–500. DOI 10.4028/www.scientific.net/AMM.692.497.
15. Katla, B., Raju, S., Waim, A. R., Danam, V. A. (2021). Utilization of higher percentages of RAP for improved mixture performance by adopting the process of fractionation. *International Journal of Pavement Research and Technology, 5(12),* 100–105.
16. Loria, L., Hajj, E. Y., Sebaaly, P. E., Barton, M., Kass, S. et al. (2011). Performance evaluation of asphalt mixtures with high recycled asphalt pavement content. *Transportation Research Record, 2208(1),* 72–81. DOI 10.3141/2208-10.
17. Wu, J. R., Niu, Z. X., Chen, H. Y. (2022). Effect of aging on low-temperature crack resistance and water stability of polyester fiber asphalt mixture. *Materials Research Express, 9(1),* 015101. DOI 10.1088/2053-1591/ac46e7.
18. Cox, B. C., Smith, B. T., Howard, I. L., James, R. S. (2017). State of knowledge for cantabro testing of dense graded asphalt. *Journal of Materials in Civil Engineering, 29(10),* 04017174. DOI 10.1061/(ASCE)MT.1943-5533.0002020.
19. Rimsa, V., Kacianauskas, R., Sivilevicius, H. (2014). Numerical analysis of asphalt mixture and comparison with physical marshall test. *Journal of Civil Engineering and Management, 20(4),* 570–580. DOI 10.3846/13923730.2014.920413.
20. Rafiq, W., Bin Napiah, M., Sutanto, M. H., Alaloul, W. S., Khan, M. I. et al. (2020). Performance evaluation for rutting and moisture damage of Hot asphalt mixtures using high percentage of recycled asphalt pavement material. In: *IOP conference series: Earth and environmental science*, vol. 498, 012010.

21. Tarefder, R. A., Weldegiorgis, M. T., Ahmad, M. (2014). Assessment of the effect of pore pressure cycles on moisture sensitivity of hot mix asphalt using MIST conditioning and dynamic modulus. *Journal of Testing and Evaluation, 42(6),* 20130095. DOI 10.1520/JTE20130095.
22. Lacroix, A., Regimand, A., James, L. (2016). Proposed approach for evaluation of cohesive and adhesive properties of asphalt mixtures for determination of moisture sensitivity. *Transportation Research Record Journal of the Transportation Research Board, 2575(1),* 61–69. DOI 10.3141/2575-07.
23. Transport, R. (2004). JTG F40-2004 standard test methods for bitumen and bituminous mixtures for highway engineering.
24. Showkat, B., Singh, D. (2022). Effect of MIST conditioning on the air voids and permeability of hot asphalt mixes containing reclaimed asphalt pavement. *Road Materials Pavement, 23(7),* 1605–1632. DOI 10.1080/14680629.2021.1910549.
25. Ahmad, M., Mannan, U. A., Islam, M. R., Tarefder, R. A. (2018). Chemical and mechanical changes in asphalt binder due to moisture conditioning. *Road Materials & Pavement Design, 19(5),* 1–14. DOI 10.1080/14680629.2017.1299631.
26. Barugahare, J., Amirkhanian, A. N., Xiao, F., Amirkhanian, S. N. (2021). Evaluation of ANN-based dynamic modulus models of asphalt mixtures. *Journal of Materials in Civil Engineering, 33(6),* 04021099. DOI 10.1061/(ASCE)MT.1943-5533.0003721.
27. Zhu, F., Guo, D. D. (2013). Influence of graduation on road performance of fibers-reinforced asphalt pavement. *Advanced Materials Research, 753–755,* 754–757. DOI 10.4028/www.scientific.net/AMR.753-755.754.
28. Kuang, D., Jiao, Y., Ye, Z., Lu, Z., Chen, H. et al. (2018). Diffusibility enhancement of rejuvenator by epoxidized soybean oil and its influence on the performance of recycled hot mix asphalt mixtures. *Materials, 11(5),* 833. DOI 10.3390/ma11050833.
29. Chen, Z. W., Gong, Z. L., Jiao, Y. Y., Wang, Y., Shi, K. et al. (2020). Moisture stability improvement of asphalt mixture considering the surface characteristics of steel slag coarse aggregate. *Construction and Building Materials, 251,* 118987. DOI 10.1016/j.conbuildmat.2020.118987.
30. Wu, H., Li, P., Nian, T., Zhang, G., He, T. et al. (2019). Evaluation of asphalt and asphalt mixtures' water stability method under multiple freeze-thaw cycles. *Construction and Building Materials, 228,* 117089. DOI 10.1016/j.conbuildmat.2019.117089.
31. Mogawer, W., Austerman, A., Roussel, M. (2013). Performance characteristics of asphalt rubber mixtures containing RAP and warm mix asphalt technology. *2nd International Warm-Mix Asphalt Conference*, vol. 10, pp. 20–23. Brasília, Brasil.